

A generalized self-consistent method for estimating effective shear properties of unidirectional composites comprising cylindrical orthotropic constituents

M Minhat*, N Z Mahmud Zuhudi, M H Shamsudin, M D Isa and M K Harun

Universiti Kuala Lumpur - Malaysian Institute of Aviation Technology, Malaysia

*mulia@unikl.edu.my

Abstract. A micromechanics model based on generalized self-consistent method is proposed to estimate shear elastic properties of unidirectional fibre composites comprising cylindrical orthotropic layers. The features of the generalized self-consistent method are briefly presented and the homogenization schemes in determining the effective shear moduli of transversely isotropic medium are demonstrated. Numerical examples on the prediction of axial and transverse shear moduli of polymer composite reinforced with nanostructure hybrid fibres are illustrated. The close agreement between the prediction results and the results obtained from the available experimental data and finite element study validates the solutions produced by the proposed model.

1. Introduction

Recent advances in nano-material sciences have led to the development of different types of advanced multifunctional composite materials, which are designed for simultaneous enhancement in various structural functions including stiffness, strength, vibrational damping, fracture, electrical and thermal conductivities [1, 2]. One of the examples of such advanced composites currently developed for such intended multi-functionality purposes is nanostructures hybrid fibres reinforced polymeric material. Basically, these fibres have radially aligned nanostructures that directly grown on the fibre surfaces. In most cases, the nanostructures are in form of nanowires and carbon nanotubes (CNTs). The presence of nanowires coated fibre have been shown to improve shear, damping and electrical characteristics of the polymeric composites when compared to the conventional fibre composite materials [3, 4, 5]. In case of carbon nanotubes, the fibre system is also known as ‘fuzzy’ fibre and similar enhancements including thermal and electrical behaviours were observed when such fibre system is embedded into polymeric materials [6-8,27]. These materials, from the practical perspective, could be very beneficial for the next generation multi-functional advanced fibre composite materials.

It is interesting to note that due to the presence of radially aligned nanostructures surrounding the main fibre, a fictitious reinforced interphase layer comprising the nanostructures and matrix material is formed. This layer is responsible for the enhancement in the shear characteristics of fibre composite material, which are well known to exhibit the poor performance for the conventional fibre reinforced composites. Therefore, it is of interest to estimate the effective shear properties of such propitious advanced composite materials.



To model the effective shear moduli of the unidirectional nanostructures hybrid fibre composite material, three distinct constituents are considered, which include base carbon fibre, polymer matrix material and reinforced interphase layer. As such, an analysis on a multiphase composite is necessary. From the material point of view, each constituent has different characteristic. Typically, the polymer matrix is modelled as an isotropic material and carbon fibre as a transversely isotropic material with axis of symmetry parallel to the principle axis of fibre. Interestingly, the reinforced interphase layer can be treated as nano-composite medium and it assumes the cylindrical orthotropic property [9, 10] considering that they are radially grown on the surface of fibre. From general modelling perspective, all constituents in such fibre composite system can be generalized to have orthotropic property where isotropic, as well as transversely isotropic property, is considered as a special case of the orthotropic property having one or more plane of material symmetry.

In the research and engineering practices, estimating the effective elastic properties of multiphase composites with known properties of the constituents is essential for initial and associated analysis. In general, such prediction requires micromechanics modelling and in the first approximation analysis, the most popular classical micromechanics models used include composite cylindrical assemblage (CCA) method [11], self-consistent method [12], generalized self-consistent (GSC) method or three-phase model [13], differential scheme [14] and also Mori-Tanaka's method [15]. The GSC method has been critically assessed and validated based on the most elusive property of transverse shear modulus, showing that estimations were most in agreement to numerical simulations and experimental data up to the typical high volume fraction of inclusion [13, 16, 17, 18, 19]. In fact, many modern analytical or semi-analytical micromechanics approaches used the results of GSC method for base comparison in justifying the accuracies of their proposed models [18, 19]. It should be noted that majority of these classical models were originally developed to homogenize the effective elastic properties of a two-phase composite having constituent to possess either isotropic or transversely isotropic property with plane of symmetry perpendicular to the principle axis of fibre. In later period, some of these models were upgraded for the multiphase composite applications, i.e. to study the effect of interphase layer, coating layer and voids [20, 21, 22].

Therefore, in this paper, the GSC method will be applied to predict the axial and transverse shear moduli of multiphase unidirectional composite system comprising cylindrical orthotropic constituents. Some mathematical preliminaries and the features of GSC method are presented. For illustrations, few numerical examples on nanowire and CNTs hybrid fibre composites are studied here and for further validation, some results are compared with the existing experimental findings and numerical studies.

2. The formulation of generalized self-consistent method

In this section, the mathematical preliminaries related to linear classical elasticity and homogenization techniques are briefly reviewed. The features and governing equations related to the GSC method are presented.

2.1. Mathematical preliminaries

Constitutive equation of Hooke's law for orthotropic linear elastic material having nine independent constants written compactly in cylindrical coordinate system can be written as Equation 1.

$$\begin{pmatrix} \sigma_{rr}^{(i)} \\ \sigma_{\theta\theta}^{(i)} \\ \sigma_{zz}^{(i)} \\ \sigma_{\theta z}^{(i)} \\ \sigma_{rz}^{(i)} \\ \sigma_{r\theta}^{(i)} \end{pmatrix} = \begin{bmatrix} C_{rr}^{(i)} & C_{r\theta}^{(i)} & C_{rz}^{(i)} & 0 & 0 & 0 \\ C_{r\theta}^{(i)} & C_{\theta\theta}^{(i)} & C_{\theta z}^{(i)} & 0 & 0 & 0 \\ C_{rz}^{(i)} & C_{\theta z}^{(i)} & C_{zz}^{(i)} & 0 & 0 & 0 \\ 0 & 0 & 0 & G_{\theta z}^{(i)} & 0 & 0 \\ 0 & 0 & 0 & 0 & G_{rz}^{(i)} & 0 \\ 0 & 0 & 0 & 0 & 0 & G_{r\theta}^{(i)} \end{bmatrix} \begin{pmatrix} \varepsilon_{rr}^{(i)} \\ \varepsilon_{\theta\theta}^{(i)} \\ \varepsilon_{zz}^{(i)} \\ 2\varepsilon_{\theta z}^{(i)} \\ 2\varepsilon_{rz}^{(i)} \\ 2\varepsilon_{r\theta}^{(i)} \end{pmatrix} \quad (1)$$

where σ_{pq} and ε_{pq} are the second order linear stress and strain tensors, respectively, and C_{pq} is the fourth-order stiffness tensors written in compact form. The superscript index is given as $i = 1, 2, \dots, N$ and N is the total number of constituents in a composite. For transversely isotropic material with its axis of symmetry parallel to z – axis, the stress-strain equation assumes the form as in Equation 2.

$$\begin{pmatrix} \sigma_{rr}^{(i)} \\ \sigma_{\theta\theta}^{(i)} \\ \sigma_{zz}^{(i)} \\ \sigma_{\theta z}^{(i)} \\ \sigma_{rz}^{(i)} \\ \sigma_{r\theta}^{(i)} \end{pmatrix} = \begin{bmatrix} C_{rr}^{(i)} & C_{r\theta}^{(i)} & C_{rz}^{(i)} & 0 & 0 & 0 \\ C_{r\theta}^{(i)} & C_{rr}^{(i)} & C_{rz}^{(i)} & 0 & 0 & 0 \\ C_{rz}^{(i)} & C_{rz}^{(i)} & C_{zz}^{(i)} & 0 & 0 & 0 \\ 0 & 0 & 0 & G_{rz}^{(i)} & 0 & 0 \\ 0 & 0 & 0 & 0 & G_{rz}^{(i)} & 0 \\ 0 & 0 & 0 & 0 & 0 & \frac{C_{rr}^{(i)} - C_{r\theta}^{(i)}}{2} \end{bmatrix} \begin{pmatrix} \varepsilon_{rr}^{(i)} \\ \varepsilon_{\theta\theta}^{(i)} \\ \varepsilon_{zz}^{(i)} \\ 2\varepsilon_{\theta z}^{(i)} \\ 2\varepsilon_{rz}^{(i)} \\ 2\varepsilon_{r\theta}^{(i)} \end{pmatrix} \quad (2)$$

where the stiffness tensor consists of five independent elastic constants only. As will be seen later, it is useful to define stiffness tensor for transversely isotropic medium with its axis of symmetry parallel to r – axis, which can be written as Equation 3.

$$\begin{pmatrix} \sigma_{rr}^{(i)} \\ \sigma_{\theta\theta}^{(i)} \\ \sigma_{zz}^{(i)} \\ \sigma_{\theta z}^{(i)} \\ \sigma_{rz}^{(i)} \\ \sigma_{r\theta}^{(i)} \end{pmatrix} = \begin{bmatrix} C_{rr}^{(i)} & C_{r\theta}^{(i)} & C_{r\theta}^{(i)} & 0 & 0 & 0 \\ C_{r\theta}^{(i)} & C_{\theta\theta}^{(i)} & C_{\theta z}^{(i)} & 0 & 0 & 0 \\ C_{r\theta}^{(i)} & C_{\theta z}^{(i)} & C_{\theta\theta}^{(i)} & 0 & 0 & 0 \\ 0 & 0 & 0 & \frac{C_{\theta\theta}^{(i)} - C_{\theta z}^{(i)}}{2} & 0 & 0 \\ 0 & 0 & 0 & 0 & G_{r\theta}^{(i)} & 0 \\ 0 & 0 & 0 & 0 & 0 & G_{r\theta}^{(i)} \end{bmatrix} \begin{pmatrix} \varepsilon_{rr}^{(i)} \\ \varepsilon_{\theta\theta}^{(i)} \\ \varepsilon_{zz}^{(i)} \\ 2\varepsilon_{\theta z}^{(i)} \\ 2\varepsilon_{rz}^{(i)} \\ 2\varepsilon_{r\theta}^{(i)} \end{pmatrix} \quad (3)$$

Finally, the stress-strain relationship for isotropic material is described by Equation 4.

$$\begin{pmatrix} \sigma_{rr}^{(i)} \\ \sigma_{\theta\theta}^{(i)} \\ \sigma_{zz}^{(i)} \\ \sigma_{\theta z}^{(i)} \\ \sigma_{rz}^{(i)} \\ \sigma_{r\theta}^{(i)} \end{pmatrix} = \begin{bmatrix} C_{rr}^{(i)} & C_{r\theta}^{(i)} & C_{r\theta}^{(i)} & 0 & 0 & 0 \\ C_{r\theta}^{(i)} & C_{rr}^{(i)} & C_{r\theta}^{(i)} & 0 & 0 & 0 \\ C_{r\theta}^{(i)} & C_{r\theta}^{(i)} & C_{rr}^{(i)} & 0 & 0 & 0 \\ 0 & 0 & 0 & \frac{C_{rr}^{(i)} - C_{r\theta}^{(i)}}{2} & 0 & 0 \\ 0 & 0 & 0 & 0 & \frac{C_{rr}^{(i)} - C_{r\theta}^{(i)}}{2} & 0 \\ 0 & 0 & 0 & 0 & 0 & \frac{C_{rr}^{(i)} - C_{r\theta}^{(i)}}{2} \end{bmatrix} \begin{pmatrix} \varepsilon_{rr}^{(i)} \\ \varepsilon_{\theta\theta}^{(i)} \\ \varepsilon_{zz}^{(i)} \\ 2\varepsilon_{\theta z}^{(i)} \\ 2\varepsilon_{rz}^{(i)} \\ 2\varepsilon_{r\theta}^{(i)} \end{pmatrix} \quad (4)$$

where only two independent elastic constants are required to fully describe such material behaviour. The Cauchy small strain-displacement written in the cylindrical coordinate system has the relations as follow.

$$\begin{aligned} \varepsilon_{rr} &= \frac{\partial u_r}{\partial r}, \quad \varepsilon_{\theta\theta} = \frac{1}{r} \left(\frac{\partial u_\theta}{\partial \theta} + u_r \right), \quad \varepsilon_{zz} = \frac{\partial u_z}{\partial z}, \\ \varepsilon_{rz} &= \frac{1}{2} \left(\frac{\partial u_z}{\partial r} + \frac{\partial u_r}{\partial z} \right), \quad \varepsilon_{\theta z} = \frac{1}{2} \left(\frac{\partial u_\theta}{\partial z} + \frac{1}{r} \frac{\partial u_z}{\partial \theta} \right), \quad \varepsilon_{r\theta} = \frac{1}{2} \left(\frac{1}{r} \frac{\partial u_r}{\partial \theta} + \frac{\partial u_\theta}{\partial r} - \frac{u_\theta}{r} \right) \end{aligned} \quad (5)$$

where u_p is displacements in respective coordinate system. Corresponding equations of equilibrium in cylindrical coordinate system are given as follows:

$$\begin{aligned}\frac{\partial \sigma_{rr}}{\partial r} + \frac{1}{r} \frac{\partial \sigma_{r\theta}}{\partial \theta} + \frac{\sigma_{rr} - \sigma_{\theta\theta}}{r} + \frac{\partial \sigma_{rz}}{\partial z} &= 0, \\ \frac{\partial \sigma_{r\theta}}{\partial r} + \frac{1}{r} \frac{\partial \sigma_{\theta\theta}}{\partial \theta} + \frac{2\sigma_{r\theta}}{r} + \frac{\partial \sigma_{\theta z}}{\partial z} &= 0, \\ \frac{\partial \sigma_{rz}}{\partial r} + \frac{1}{r} \frac{\partial \sigma_{\theta z}}{\partial \theta} + \frac{\sigma_{rz}}{r} + \frac{\partial \sigma_{zz}}{\partial z} &= 0.\end{aligned}\quad (6)$$

Most micromechanics methods employ energy principle in homogenizing the heterogeneous properties of composite materials. Thus, it is necessary to describe the relationship between energy, stress and strain in linear elastic material, which can be represented as in Equation 7.

$$W(\epsilon_{pq}) = \frac{1}{2} \sigma_{pq} \epsilon_{pq} = \frac{1}{2} C_{pqrs} \epsilon_{rs} \epsilon_{pq} \quad (7)$$

where W designates the strain energy density in a material.

The concept of representative volume element (RVE) is commonly used in many micromechanics models. RVE can be thought as the smallest possible unit volume element over which homogenization takes place and the average properties are obtained to represent the effective properties of a whole material. It should be noted that RVE must be carefully chosen in such a way that its size is notably large enough to account for sufficient number of various nanostructures but extremely small compared to the size of a whole composite material so that accurate estimation of the effective properties can be achieved. Furthermore, such RVE size requirement is also required for the effective properties to be independent of the surface values of displacement or traction vector as long as these values remain macroscopically homogeneous [12]. In addition, any quantity measured inside the RVE is considered as an average value and this value is normally represented by $\langle \bullet \rangle = \frac{1}{V} \int_V (\bullet) dV$ where V is the volume of RVE. For example, the respective average strain energy density, strain and stress in RVE can be written as:

$$\langle W \rangle = \frac{1}{2V} \int_V \sigma_{pq} \epsilon_{pq} dV, \quad \langle \epsilon_{pq} \rangle = \frac{1}{V} \int_V \epsilon_{pq} dV, \quad \langle \sigma_{pq} \rangle = \frac{1}{V} \int_V \sigma_{pq} dV. \quad (8)$$

Furthermore, with the presence of ideal contact surface between the constituents and macroscopically uniform boundary conditions, the respective average strain and stress in the RVE is identical to the respective homogenous strain and stress applied on its boundary, for example:

$$\langle \epsilon_{pq} \rangle = \epsilon_{pq}^0, \quad \langle \sigma_{pq} \rangle = \sigma_{pq}^0 \quad (9)$$

where ϵ_{pq}^0 and σ_{pq}^0 are the homogenous strain and stress applied on the boundary surface of RVE respectively, which are also equal to the macroscopically homogenous boundary conditions imposed on the macroscopic composite material. Equalities shown in Equation 9 are known as the average strain and average stress theorems respectively.

Finally, in averaging the final properties of unidirectional fibre composite material, the fibres are typically assumed as infinitely long cylinders with circular cross-section and they are also randomly distributed within the composite ply. In this approach, the principle axis of fibre is oriented to z-axis as such transversely isotropic composite with its plane of the symmetry perpendicular to z-axis is obtained. In this case, the behaviour of such composite system can be defined by five effective engineering moduli, which include plane strain bulk modulus κ_{12}^{eff} , axial Young's modulus E_{33}^{eff} ,

major Poisson's ratio ν_{31}^{eff} , axial shear modulus μ_{23}^{eff} and transverse shear modulus μ_{12}^{eff} . Nevertheless, in this paper, only the shear properties are of concern.

2.2. The generalized self-consistent method

The GSC method employs RVE based on the physical model adopted from the composite cylindrical assemblage (CCA) method [11] where it contains single inclusion of fibre only embedded in a matrix system in the form of concentric cylinders. However, RVE in the GSC formulation treats fibre, matrix and, in this case, reinforced interphase layer as inclusions. These inclusions in concentric cylindrical assemblage form is surrounded by an equivalent homogenized medium having unknown properties that we wish to determine. Such RVE can be considered as a multi-layered or N - layered cylindrical orthotropic unidirectional composite system (see Figure 1a). In this study, $N = 3$ where the fibre is designated by $i = 1$, $i = 2$ for reinforced interphase layer and for matrix, $i = 3$. Naturally, the fibre volume fraction can be defined as the ratio of circumferential areas of the fibre over matrix, i.e. $V_f = r_1^2 / r_N^2$. As for the equivalent homogenized medium, it is designated by $N + 1$ and has an infinite outer radius where homogenous deformation is imposed.

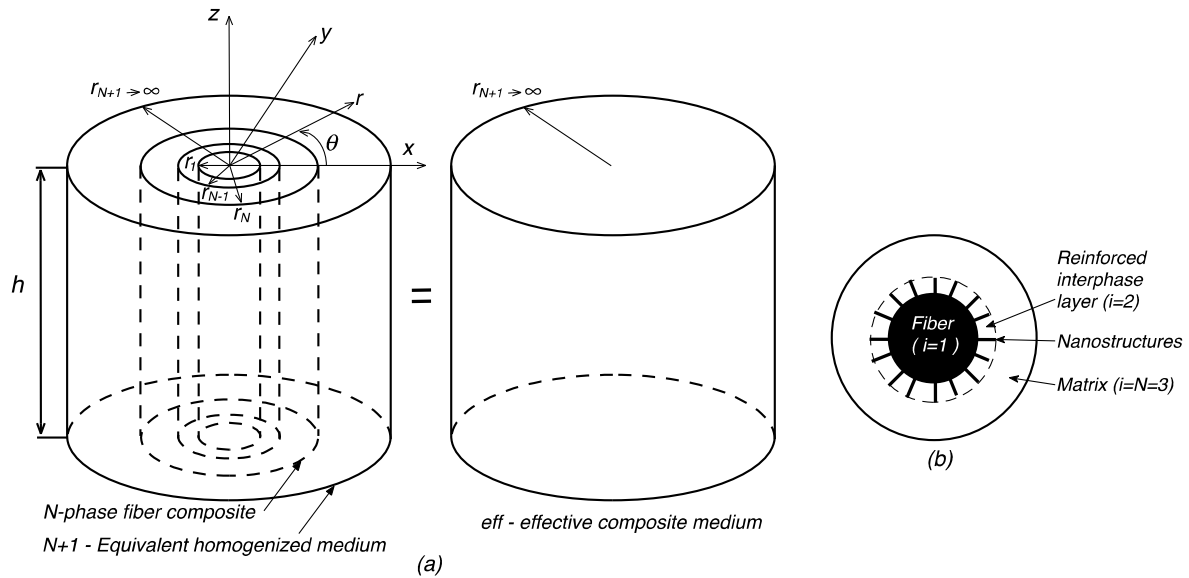


Figure 1. Schematic RVEs of (a) cylindrical composite assemblage in the GSC method and (b) nanostructures hybrid fibre composite

The GSC method originally proposed by Christensen and Lo [13] was developed on the basis of energy principle. It is important for us to understand first that, when the RVE containing the inclusions is homogenized, the homogenized RVE can be represented as an effective composite medium, which is designated as *eff* -medium and this medium also has the same unknown effective properties of the equivalent homogenized medium, i.e. $\mu_{23}^{N+1} = \mu_{23}^{eff}$ and $\mu_{12}^{N+1} = \mu_{12}^{eff}$. The equivalent RVE for effective composite medium is as shown in Figure 1a. Based on the energy principle, it is proposed that the difference in average strain energy densities of RVE containing inclusions and RVE of an effective composite medium equals

$$\langle W^{RVE} \rangle = \langle W^{eff} \rangle + \langle W^{INT} \rangle = \langle W^{eff} \rangle + \frac{1}{2V} \int_S \left(\sigma_{ij}^{N+1} u_j^{eff} - \sigma_{ij}^{eff} u_j^{N+1} \right) dS \quad (10)$$

where $\langle W^{RVE} \rangle$ is the average strain energy density of a medium or RVE with inclusions, $\langle W^{eff} \rangle$ is the average strain energy density of a medium without the inclusion or RVE of an effective composite medium, $\langle W^{INT} \rangle$ is the average surface interaction strain energy density at contact surface S between the N^{th} –layer and $(N+1)^{th}$ –layer, $\sigma_{pq}^{N+1}, u_q^{N+1}$ are the components of stress tensor and displacement vector on the contact surface of $(N+1)^{th}$ –medium respectively, $\sigma_{pq}^{eff}, u_q^{eff}$ assume the respective stress tensor and displacement vector on the contact surface of an effective composite medium. Christensen and Lo [13] further postulated that the average strain energy densities of RVE containing the inclusions and RVE of an effective composite medium are equal (see Equation 11).

$$\langle W^{RVE} \rangle = \langle W^{eff} \rangle \quad (11)$$

Using Equation 11, Equation 10 is reduced to:

$$\frac{1}{2V} \int_S \left(\sigma_{pq}^{N+1} u_q^{eff} - \sigma_{pq}^{eff} u_q^{N+1} \right) dS = 0. \quad (12)$$

It can be concluded that Equation 12 appears as a result of average strain energy density equivalency between medium with inclusions and effective medium. The importance of this equation will be illustrated in the next section when solving for the unknown effective shear moduli.

3. Homogenization schemes in the GSC method

In this section, the homogenization procedures based on GSC method in determining the effective axial and transverse shear moduli are demonstrated.

3.1. Effective axial shear modulus

The allowable displacement field that satisfies equilibrium equations under specific axial shear loading deformation applied at outer boundaries of RVE for every orthotropic phase can be written in the form of Equation 13.

$$u_z^{(i)}(r, \theta) = \left(D_1^{(i)} r^{\lambda_{(i)}} + D_2^{(i)} r^{-\lambda_{(i)}} \right) \cos \theta \quad (13)$$

where index i identifies the phase in RVE, $D_1^{(i)}$ and $D_2^{(i)}$ are the unknown constants associated with each phase or layer in a composite (see Appendix A.1) and $\lambda_{(i)} = \sqrt{G_{\theta z}^{(i)} / G_{rz}^{(i)}}$ is a material constant related to the material property of that particular phase, i.e. $\lambda_{(i)}$ equals 1 for isotropic and transversely isotropic material plane of isotropy perpendicular to the principle axis of main fibre.

Substituting Equation 13 into Equation 5 and subsequently, into Equation 6, the allowable stress fields for every orthotropic phase can be obtained, which are written as:

$$\begin{aligned} \sigma_{\theta z}^{(i)}(r, \theta) &= -G_{\theta z}^{(i)} \left(D_1^{(i)} r^{\lambda_{(i)}-1} + D_2^{(i)} r^{-\lambda_{(i)}-1} \right) \sin \theta, \\ \sigma_{rz}^{(i)}(r, \theta) &= G_{rz}^{(i)} \left(\lambda_{(i)} D_1^{(i)} r^{\lambda_{(i)}-1} - \lambda_{(i)} D_2^{(i)} r^{-\lambda_{(i)}-1} \right) \cos \theta. \end{aligned} \quad (14)$$

For $(N+1)$ –medium, which possesses transversely isotropic property with its plane of isotropy perpendicular to the principle axis of main fibre, Equation 13 and Equation 14 transform into:

$$u_z^{N+1}(r, \theta) = \left(D_1^{N+1} r + D_2^{N+1} r^{-1} \right) \cos \theta, \quad (15)$$

$$\begin{aligned} \sigma_{\theta z}^{N+1}(r, \theta) &= -\mu_{23}^{N+1} \left(D_1^{N+1} + D_2^{N+1} r^{-2} \right) \sin \theta, \\ \sigma_{rz}^{N+1}(r, \theta) &= \mu_{23}^{N+1} \left(D_1^{N+1} - D_2^{N+1} r^{-2} \right) \cos \theta. \end{aligned} \quad (16)$$

Notice that Equation 16 contains the unknown effective axial shear modulus μ_{23}^{N+1} that is intended to be determined. Since $N = 3$, a total of eight unknown constants with one unknown effective shear modulus must be determined - $D_1^{(1)}, D_2^{(1)}, D_1^{(2)}, D_2^{(2)}, D_1^{(3)}, D_2^{(3)}, D_1^{N+1}, D_2^{N+1}$ and μ_{23}^{N+1} .

Initially, it is imperative to understand that the solution to this boundary problem ceases to exist at the origin $r_0 = 0$. Thus, for the solution to exist the non-singularity condition must be obeyed such that the second unknown constant of the first layer must vanish, i.e. $D_2^{(1)} = 0$. Subsequently, the remaining seven unknown constants and one unknown effective modulus are determined from the continuity conditions at ideal contact surfaces between the phases:

$$\begin{aligned} u_z^{(i)}(r_{(i)}, \theta) &= u_z^{(i+1)}(r_{(i)}, \theta), \quad (i = 1, 2, \dots, N) \\ \sigma_{rz}^{(i)}(r_{(i)}, \theta) &= \sigma_{rz}^{(i+1)}(r_{(i)}, \theta), \end{aligned} \quad (17)$$

and from the external boundary condition imposed at outer radius of RVE ($r_{N+1} \rightarrow \infty$):

$$u_z^{N+1}(r_{N+1}) = 2\varepsilon_0 r_{N+1} \cos \theta \quad (18)$$

and finally, from the surface integral equation given by Equation 8:

$$\int_S \left(\sigma_{rz}^{N+1} u_z^{eff} - \sigma_{rz}^{eff} u_z^{N+1} \right)_{r=r_N} dS = 0 \quad (19)$$

To integrate Equation 19, the displacement and stress fields for effective composite medium need to be defined first. Prior to that, it must be emphasized that the admissible displacement and stress fields for $(N+1)$ -medium are also applicable to effective composite medium where the superscript $N+1$ is simply replaced by *eff*. Furthermore, the non-singularity solution requirement as well as the imposed external boundary condition of Equation 18 are also applicable to that composite medium; as such based on Equation 15 and Equation 16, the required displacement and stress fields for effective composite medium can be written as:

$$\begin{aligned} u_z^{eff}(r, \theta) &= D_1^{eff} \cos \theta, \\ \sigma_{\theta z}^{eff}(r, \theta) &= -\mu_{23}^{eff} D_1^{eff} \sin \theta, \\ \sigma_{rz}^{eff}(r, \theta) &= \mu_{23}^{eff} D_1^{eff} \cos \theta. \end{aligned} \quad (20)$$

It easy to show that with Equation 16, Equation 18 and Equation 20, the integration of Equation 19 leads to $D_2^{(N+1)} = 0$ and subsequently, by Equation 15 and Equation 18, $D_1^{(N+1)} = 2\varepsilon_0$. Finally, the six remaining unknowns including the effective axial shear modulus $\mu_{23}^{eff} = \mu_{23}^{N+1}$ can now be solved from the six simultaneous equations generated from Equation 17, which are listed as follows:

$$\begin{aligned} 1) \quad & D_1^{(1)} r_1^{\lambda_{(1)}} - D_1^{(2)} r_1^{\lambda_{(2)}} - D_2^{(2)} r_1^{-\lambda_{(2)}} = 0, \\ 2) \quad & D_1^{(2)} r_2^{\lambda_{(2)}} + D_2^{(2)} r_2^{-\lambda_{(2)}} - D_1^{(3)} r_2^{\lambda_{(3)}} - D_2^{(3)} r_2^{-\lambda_{(3)}} = 0, \\ 3) \quad & D_1^{(3)} r_3^{\lambda_{(3)}} + D_2^{(3)} r_3^{-\lambda_{(3)}} - 2\varepsilon_0 r_3 = 0, \\ 4) \quad & C_{55}^{(1)} \lambda_{(1)} D_1^{(1)} r_1^{\lambda_{(1)}-1} - C_{55}^{(2)} \lambda_{(2)} D_1^{(2)} r_1^{\lambda_{(2)}-1} + C_{55}^{(2)} \lambda_{(2)} D_2^{(2)} r_1^{-\lambda_{(2)}-1} = 0, \\ 5) \quad & C_{55}^{(2)} \lambda_{(2)} D_1^{(2)} r_2^{\lambda_{(2)}-1} - C_{55}^{(2)} \lambda_{(2)} D_2^{(2)} r_2^{-\lambda_{(2)}-1} - C_{55}^{(3)} \lambda_{(3)} D_1^{(3)} r_2^{\lambda_{(3)}-1} + C_{55}^{(3)} \lambda_{(3)} D_2^{(3)} r_2^{-\lambda_{(3)}-1} = 0, \\ 6) \quad & C_{55}^{(3)} \lambda_{(3)} D_1^{(3)} r_3^{\lambda_{(3)}-1} - C_{55}^{(3)} \lambda_{(3)} D_2^{(3)} r_3^{-\lambda_{(3)}-1} - 2\varepsilon_0 \mu_{23}^{N+1} = 0. \end{aligned} \quad (21)$$

It is interesting to point out that the last expression shown in Equation 21 gives explicit expression for final effective axial shear modulus and this can be rewritten as Equation 22.

$$\mu_{23}^{eff} = \frac{1}{2\varepsilon_0} C_{55}^{(N)} \left[\lambda_{(N)} D_1^{(N)} r^{\lambda_{(N)}-1} + (-\lambda_{(N)}) D_2^{(N)} r^{-\lambda_{(N)}-1} \right], \quad (22)$$

where $\lambda_{(N)} = \sqrt{G_{\theta z}^{(N)} / G_{rz}^{(N)}}$. It is possible to get different expression of effective modulus from the one obtained in Equation 22, and this is obtained through Equation 10 or Equation 11. With the help of Equation 7 and Equation 8, the term on the left hand-side of Equation 11 leads to:

$$\langle W^{eff} \rangle = \frac{1}{2V} \int_V \sigma_{pq}^{eff} \varepsilon_{pq}^{eff} dV = 2\mu_{23}^{eff} \varepsilon_0^2 \quad (23)$$

while the term on the right hand-side gives

$$\langle W^{RVE} \rangle = \frac{1}{2r_{N+1}^2} \left[\sum_{i=1}^N C_{44}^{(i)} \left(\frac{(D_1^{(i)})^2}{\lambda_{(i)}} (r_{(i)}^{2\lambda_{(i)}} - r_{(i-1)}^{2\lambda_{(i)}}) + \frac{(D_2^{(i)})^2}{-\lambda_{(i)}} (r_{(i)}^{-2\lambda_{(i)}} - r_{(i-1)}^{-2\lambda_{(i)}}) \right) + 4\mu_{23}^{N+1} \varepsilon_0^2 r_{N+1}^2 - 4\mu_{23}^{N+1} \varepsilon_0^2 r_N^2 \right]. \quad (24)$$

Thus, equating Equation 23 and Equation 24 yields

$$\mu_{23}^{eff} = \frac{1}{4(\varepsilon_0 r_N)^2} \sum_{i=1}^N C_{44}^{(i)} \left(\frac{(D_1^{(i)})^2}{\lambda_{(i)}} (r_{(i)}^{2\lambda_{(i)}} - r_{(i-1)}^{2\lambda_{(i)}}) + \frac{(D_2^{(i)})^2}{-\lambda_{(i)}} (r_{(i)}^{-2\lambda_{(i)}} - r_{(i-1)}^{-2\lambda_{(i)}}) \right). \quad (25)$$

Although the expressions found in Equation 22 and Equation 25 are different, they produce identical results when numerical calculations are performed.

3.2. Effective transverse shear modulus

The admissible displacement fields for each orthotropic layer under specific transverse shear loading condition imposed at the outer radius of RVE can be written as

$$\begin{aligned} u_r^{(i)}(r) &= \left(\phi_1^{(i)} D_1^{(i)} r^{\lambda_1^{(i)}} + \phi_2^{(i)} D_2^{(i)} r^{\lambda_2^{(i)}} + \phi_3^{(i)} D_3^{(i)} r^{\lambda_3^{(i)}} + \phi_4^{(i)} D_4^{(i)} r^{\lambda_4^{(i)}} \right) \sin 2\theta, \\ u_\theta^{(i)}(r) &= \left(D_1^{(i)} r^{\lambda_1^{(i)}} + D_2^{(i)} r^{\lambda_2^{(i)}} + D_3^{(i)} r^{\lambda_3^{(i)}} + D_4^{(i)} r^{\lambda_4^{(i)}} \right) \cos 2\theta. \end{aligned} \quad (26)$$

where

$$\phi_j^{(i)} = 2 \left(C_{\theta\theta}^{(i)} + G_{r\theta}^{(i)} - \lambda_j^{(i)} (C_{r\theta}^{(i)} + G_{r\theta}^{(i)}) \right) \left(C_{\theta\theta}^{(i)} + 4G_{r\theta}^{(i)} - (\lambda_j^{(i)})^2 C_{rr}^{(i)} \right)^{-1} \quad (27)$$

and the material constants $\lambda_j^{(i)}$ are obtained from the following characteristic equation, which is given as

$$T(\lambda_j^{(i)})^4 - U(\lambda_j^{(i)})^2 + V = 0 \quad (28)$$

where

$$\begin{aligned} T &= C_{rr}^{(i)} G_{r\theta}^{(i)}, \\ U &= \left(C_{rr}^{(i)} + C_{\theta\theta}^{(i)} - 8C_{r\theta}^{(i)} \right) G_{r\theta}^{(i)} + 4 \left(C_{rr}^{(i)} C_{\theta\theta}^{(i)} - (C_{r\theta}^{(i)})^2 \right), \\ V &= 9C_{\theta\theta}^{(i)} G_{r\theta}^{(i)}. \end{aligned}$$

Here, it is noted that real positive values are obtained for $\lambda_1^{(i)}$ and $\lambda_3^{(i)}$ and real negative values are for $\lambda_2^{(i)}$ and $\lambda_4^{(i)}$.

Similarly as before, with Equation 5, Equation 6, Equation 26, Equation 27 and Equation 28, and the corresponding allowable stress fields for every orthotropic layer can be obtained as:

$$\begin{aligned} \sigma_{\theta\theta}^{(i)}(r) &= \left(\sum_{j=1}^4 D_j^{(i)} r^{\lambda_j^{(i)}-1} \left(C_{r\theta}^{(i)} \phi_j^{(i)} \lambda_j^{(i)} + C_{\theta\theta}^{(i)} (\phi_j^{(i)} - 2) \right) \right) \sin 2\theta, \\ \sigma_{r\theta}^{(i)}(r) &= G_{r\theta} \left(\sum_{j=1}^4 D_j^{(i)} r^{\lambda_j^{(i)}-1} \left(2\phi_j^{(i)} + \lambda_j^{(i)} - 1 \right) \right) \cos 2\theta. \end{aligned} \quad (29)$$

For $N+1$ medium, the admissible displacement and stress fields are found as:

$$u_r^{N+1}(r, \theta) = \frac{1}{4\mu_{12}^{N+1}} \left(2r + (\eta^{N+1} + 1) D_2^{N+1} r^{-1} + D_4^{N+1} r^{-3} \right) \sin 2\theta, \quad (30)$$

$$\begin{aligned} u_\theta^{N+1}(r, \theta) &= \frac{1}{4\mu_{12}^{N+1}} \left(2r + (\eta^{N+1} - 1) D_2^{N+1} r^{-1} - D_4^{N+1} r^{-3} \right) \cos 2\theta, \\ \sigma_{rr}^{N+1}(r, \theta) &= \left(1 - \Gamma^{N+1} D_2^{N+1} r^{-2} - \frac{3}{2} D_4^{N+1} r^{-4} \right) \sin 2\theta, \\ \sigma_{r\theta}^{N+1}(r, \theta) &= \left(1 + D_2^{N+1} r^{-2} + \frac{3}{2} D_4^{N+1} r^{-4} \right) \cos 2\theta \end{aligned} \quad (31)$$

where $\eta^{N+1} = 1 + 2K_{12}^{N+1}/\mu_{12}^{N+1}$, $\Gamma^{N+1} = 1 + (K_{12}^{N+1}/\mu_{12}^{N+1})^2$.

In deriving the expressions shown in Equation 30 and Equation 31, the following equalities for unknown constants of $D_1^{N+1} = 1/2\mu_{12}^{N+1}$ and $D_3^{N+1} = 0$ were obtained. Furthermore, the unknown constants of $D_2^{(1)}$ and $D_4^{(1)}$ must also vanish due to the requirement of non-singularity solution at origin, i.e. $D_2^{(1)} = D_4^{(1)} = 0$. As before, necessary simultaneous equations need to be established to solve for twelve unknown constants — $D_1^{(1)}, D_3^{(1)}, D_1^{(2)}, D_2^{(2)}, D_3^{(2)}, D_4^{(2)}, D_1^{(3)}, D_2^{(3)}, D_3^{(3)}, D_4^{(3)}, D_2^{N+1}, D_4^{N+1}$ and one unknown desired effective modulus of $\mu_{12}^{N+1} = \mu_{12}^{eff}$. It should be noted that although the unknown effective plane strain bulk modulus ($K_{12}^{N+1} = K_{12}^{eff}$) appears in Equation 30 and Equation 31, the knowledge of such modulus is not required. To eliminate the unwanted effective modulus from system of equations, the surface integral equation is employed, which is given as Equation 32.

$$\int_S \left(\sigma_{rr}^{N+1} u_r^{eff} + \sigma_{r\theta}^{N+1} u_\theta^{eff} - \sigma_{rr}^{eff} u_r^{N+1} - \sigma_{r\theta}^{eff} u_\theta^{N+1} \right)_{r=r_N} dS = 0. \quad (32)$$

Note again that Equation 30 and Equation 31 as well as the requirement of non-singularity condition are also valid for effective composite medium; as such the allowable displacement and stress fields for such medium can be expressed as:

$$\begin{aligned} u_r^{eff}(r, \theta) &= \frac{r}{2\mu_{12}^{eff}} \sin 2\theta, & u_\theta^{eff}(r, \theta) &= \frac{r}{2\mu_{12}^{eff}} \cos 2\theta, \\ \sigma_{rr}^{eff}(r, \theta) &= \sin 2\theta, & \sigma_{r\theta}^{eff}(r, \theta) &= \cos 2\theta. \end{aligned} \quad (33)$$

Using Equation 30, Equation 31 and Equation 33, the surface integral of Equation 32 gives $D_2^{N+1} = 0$, which will then eliminate the unnecessary effective modulus from the equations. Hence, the remaining twelve unknowns including the effective transverse shear modulus can now be found with the help of continuity conditions at every perfect contact surface between phases:

$$\begin{aligned} u_r^{(i)}(r_{(i)}, \theta) &= u_r^{(i+1)}(r_{(i)}, \theta), & u_\theta^{(i)}(r_{(i)}, \theta) &= u_\theta^{(i+1)}(r_{(i)}, \theta), \\ \sigma_{rr}^{(i)}(r_{(i)}, \theta) &= \sigma_{rr}^{(i+1)}(r_{(i)}, \theta), & \sigma_{r\theta}^{(i)}(r_{(i)}, \theta) &= \sigma_{r\theta}^{(i+1)}(r_{(i)}, \theta), \quad (i = 1, 2, \dots, N); \end{aligned} \quad (34)$$

It can be seen that Equation 34 provides twelve necessary equations to solve for effective transverse shear modulus. Nevertheless, no explicit expression can be found since the established formulations in

this loading case contain nonlinear equations. As a result, an iterative method is required to solve for the unknown constants and effective modulus.

4. Numerical examples and discussions

In previous section, the homogenization schemes employed by GSC method in determining the effective axial and transverse shear properties of unidirectional fibre composite comprising cylindrical orthotropic constituents were shown. To demonstrate the capability of such method to predict the required effective properties, two problems involving different types of multifunctional advanced nanostructures hybrid fibre composites will be given. As mentioned earlier, to validate the solutions of the proposed applied model, the obtained results will be compared to the available experimental data and the results of finite element studies found in the existing literatures.

The first problem involves the estimation of effective shear properties of zinc oxide (ZnO) nanowires hybrid IM7 carbon fibre reinforced with epoxy polymer and in the second problem, the effective shear moduli of CNTs hybrid T65 carbon fibre reinforced epoxy composite are analysed. In either case, the RVE for modelling purpose comprises of four layers of fibre, reinforced interphase layer, matrix material and equivalent homogenized medium. As has been mentioned earlier, carbon fibre is normally assumed as a transversely isotropic material with its plane of isotropy perpendicular to the principle axis of fibre and physically, the properties are defined by five engineering constants, which are experimentally and/or numerically determined. From those physical properties, five elastic constants can be derived and used in the stiffness tensor shown in Equation 2. The transformation equations from physical engineering constant to elastic constants are given in the Appendix B. As for reinforced interphase layer, it exhibits cylindrically orthotropic property; however, transversely isotropic property with plane of isotropy perpendicular to principle axis of nanostructure is assumed in this analysis for simplicity. As such, the stiffness tensor shown in Equation 3 is applicable to this material. Nevertheless, this interphase layer is a composite layer, which its final properties must be obtained first through homogenization based on the properties of nanostructures and matrix material. The method and formula in determining the required effective moduli will be described next prior to numerical examples on each problem. Once the effective engineering properties are found, then the necessary elastic stiffness constants can be determined. In the case of epoxy polymer, the stiffness tensor shown in Equation 4 is applicable.

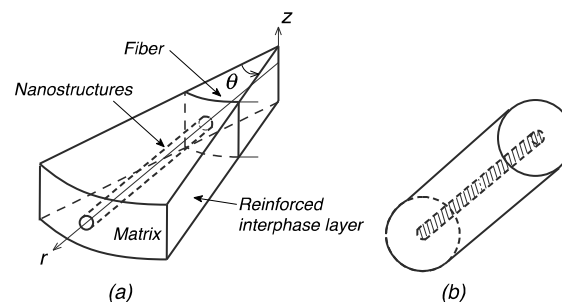


Figure 2. The RVE of (a) reinforced interphase layer and (b) equivalent geometrical model

4.1. Effective properties of reinforced interphase layer

Actual RVE of reinforced interphase layer is shown in Figure 2a and it indicates the layer has gradient property along the length of nanostructures. Nevertheless, for ease of analysis, the actual RVE can be approximated into an equivalent geometrical model as illustrated in Figure 2b. Such approach is acceptable considering the relatively small thickness of reinforced interphase layer. Here, the reinforced interphase layer is considered as a two-phase composite material where both constituents behave as isotropic material. Thus, the following commonly used formula based on the CCA and GSC methods can be used to estimate the effective transversely isotropic property of reinforced interphase

layer where the following effective properties are defined: axial Young's modulus $E_{11}^{eff-Int}$, Poisson's ratio $\nu_{12}^{eff-Int}$, plane strain bulk modulus $K_{23}^{eff-Int}$, axial shear modulus $\mu_{12}^{eff-Int}$ and transverse shear modulus $\mu_{23}^{eff-Int}$:

$$\begin{aligned}
 E_{11}^{eff-Int} &= c_b E_b + (1 - c_b) E_m + \frac{4c_b(1 - c_b)(\nu_b - \nu_m)^2 \mu_m}{(1 - c_b)\mu_m/(k_b + \mu_b/3) + c_b\mu_m/(k_m + \mu_m/3) + 1}, \\
 \nu_{12}^{eff-Int} &= c_b \nu_b + (1 - c_b) \nu_m + \frac{c_b(1 - c_b)(\nu_b - \nu_m)(\mu_m/(k_m + \mu_m/3) - \mu_m/(k_b + \mu_b/3))}{(1 - c_b)(\mu_m/(k_b + \mu_b/3)) + c_b(\mu_m/(k_m + \mu_m/3)) + 1}, \\
 K_{23}^{eff-Int} &= k_m + \frac{\mu_m}{3} + \frac{c_b}{1/(k_b - k_m + \frac{1}{3}(\mu_b - \mu_m)) + (1 - c_b)/(k_m + 4\mu_m/3)}, \\
 \frac{\mu_{12}^{eff-Int}}{\mu_m} &= \frac{\mu_b(1 + c_b) + \mu_m(1 - c_b)}{\mu_b(1 - c_b) + \mu_m(1 + c_b)}, \\
 A\left(\frac{\mu_{23}^{eff-Int}}{\mu_m}\right)^2 + 2B\left(\frac{\mu_{23}^{eff-Int}}{\mu_m}\right) + C &= 0
 \end{aligned} \tag{35}$$

where E = Young's modulus, μ = shear modulus, ν = Poisson's ratio, k = bulk modulus, c = volume fraction, $\eta = 3 - 4\nu$, and the subscripts b and m represents nanostructures and matrix, respectively, with:

$$\begin{aligned}
 A &= 3c_b(1 - c_b)^2(\mu_b/\mu_m - 1)(\mu_b/\mu_m - \eta_b) + \\
 &\quad + \left[\mu_b/\mu_m \eta_m + \eta_b \eta_m - (\eta_m \mu_b/\mu_m - \eta_b) c_b^3 \right] \left[c_b \eta_m (\mu_b/\mu_m - 1) - (\eta_m \mu_b/\mu_m + 1) \right], \\
 B &= -3c_b(1 - c_b)^2(\mu_b/\mu_m - 1)(\mu_b/\mu_m + \eta_b) + \\
 &\quad + \frac{1}{2} \left[\eta_m \mu_b/\mu_m + (\mu_b/\mu_m - 1) c_b + 1 \right] \left[(\eta_m - 1)(\mu_b/\mu_m + \eta_b) - \right. \\
 &\quad \left. - 2(\eta_m \mu_b/\mu_m - \eta_b) c_b^3 \right] + \frac{c_b}{2} (\eta_m + 1)(\mu_b/\mu_m - 1) \left[\mu_b/\mu_m + \eta_b + (\eta_m \mu_b/\mu_m - \eta_b) c_b^3 \right], \\
 C &= 3c_b(1 - c_b)^2(\mu_b/\mu_m - 1)(\mu_b/\mu_m + \eta_b) + \\
 &\quad + \left[\eta_m \mu_b/\mu_m + (\mu_b/\mu_m - 1) c_b + 1 \right] \left[\mu_b/\mu_m + \eta_b + (\eta_m \mu_b/\mu_m - \eta_b) c_b^3 \right].
 \end{aligned}$$

The volume fraction of nanostructures in this case is defined as:

$$c_b = M_b^2 d_b^2 / 4\pi(l_b + D)D \tag{36}$$

where M_b is the allowable number of nanostructures grown radially on the surface of fibre, d_b is the diameter of nanostructures, l_b is the length of nanostructures and D is the diameter of fibre. It is interesting to note such approximate model with Equation 35 and Equation 36 can be used to analysed the effects of length, diameter, density of nanostructures on the effective properties of such hybrid fibre composite material [22, 23].

4.2. Effective shear moduli of ZnO nanowires hybrid fibre composite

The configurations of the constituents used in this test problem are as follows: IM7 carbon fiber with diameter of 5.2 μm , high-density fully coated ZnO nanowires (NWs) with diameter of 50 nm and length of 500 nm, and epoxy matrix material. The mechanical properties of the constituents are derived from the work of Lurie et al [22]. The effective axial and transverse shear moduli found from the proposed method are depicted in Figure 3. As can be seen, the presence of ZnO NWs significantly enhanced the shear characteristics of such composite when compared to the properties of composite without the nanostructures. At 50% fiber volume fraction, the axial and transverse shear modulus are improved by 53% and 56% respectively. Specifically on the effective axial shear modulus, the proposed developed model gives accurate estimations on the effective property when compared to experimental data produced by Ehlert [25] for both composite having 50% fibre concentration with and without the ZnO NWs. Unfortunately, no experimental data is found on transverse shear modulus for proper comparison.

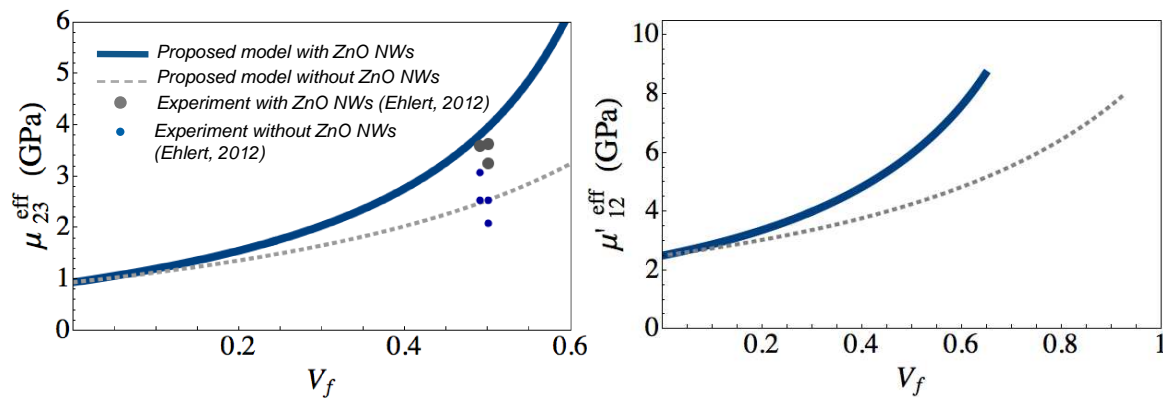


Figure 3. Estimation of (a) effective axial shear modulus, μ_{23}^{eff} and (b) effective transverse shear modulus, μ_{12}^{eff} of ZnO nanowires hybrid fibre and conventional fibre reinforced composites

4.3. Effective shear moduli of fuzzy fibre composite

In this test problem, the fuzzy fibre composite comprises T650 carbon fibre, Epikote 862 epoxy polymer and single-walled CNTs. The configurations and mechanical properties of the constituents used in this test problem are obtained from the work of Chatzigeorgiou et. al. [26]. In their work, a final element model based on asymptotic homogenization method was developed to study the effective properties of such composite system. The RVE employed in their work is based on hexagonal unit cell, which closely simulate random distribution of fibre within the composite [11]. The comparison in axial and transverse shear values is depicted in Table 1. It can be seen that the analytical results are in excellent agreement with the results produced by finite element modelling.

Table 1. Comparison on the effective properties of fuzzy fiber composites

Model	Axial shear modulus (GPa)	Transverse shear modulus (GPa)
Analytical-GSCM	2.43	7.05
FE-Hexagonal [26]	2.55	6.92

5. Conclusions

This paper presents the estimation of the effective axial and transverse shear moduli of cylindrical orthotropic composite based on the generalized self-consistent method. The concepts, features and procedures of GSCM in solving such problem are also presented. The applied model has the capability to solve the cylindrical multi-layered composites problem with isotropic, transversely isotropic and orthotropic constituents.

In estimating the effective properties, the admissible displacement fields for the two loading cases of axial and transverse shear deformation are described, from which the stress fields can be obtained. Each expression of these fields contains a set of unknown constants possessing unique values for each phase and one of the stress fields contains the respective effective shear properties. These constants, together with effective modulus, are determined with the help of non-singularity provision, continuity requirements, boundary conditions and surface integral equation derived from the GSC method. Explicit expression for the effective axial shear modulus was obtained but not for the transverse shear modulus.

Several test problems are performed and the results are evaluated and validated against available the existing data, both experimentally and numerically. It is found that the proposed model is capable to capture the behaviour of nanostructures hybrid fibre composites and predict the effective elastic properties of ZnO nanowires hybrid fibre and fuzzy fibre composites reliably and accurately.

6. Appendices

A. Derivation of admissible displacement vectors

In this appendix section, the derivations of admissible displacement fields for every constituent in the RVE are shown for axial and transverse shear loading condition cases.

A.1. Axial shear deformation

Figure A.1 illustrates the axial shear loading condition experienced by RVE where axial shear deformation is imposed at its outer boundary. It is assumed that the only solution of displacement function can exist in such loading condition is $u_z(r, \theta) \neq 0$ while $u_r = u_\theta = 0$.

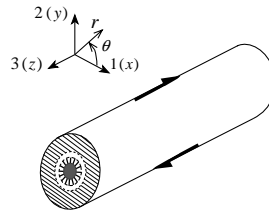


Figure A.1. Axial shear loading condition

Next, the general solution of displacement function is substituted into Equation 5, from which the following strain-displacement functions are obtained

$$\varepsilon_{zz} = \partial u_z / \partial z, \quad 2\varepsilon_{\theta z} = \frac{1}{r} \partial u_z / \partial \theta, \quad 2\varepsilon_{rz} = \partial u_z / \partial r. \quad (\text{A.1})$$

Substituting Equation A.1 into Equation 1, the stress-strain functions are found to be

$$\sigma_{\theta z} = G_{\theta z} \left(\frac{1}{r} \partial u_z / \partial \theta \right), \quad \sigma_{rz} = G_{rz} \left(\partial u_z / \partial r \right). \quad (\text{A.2})$$

Finally, rearranging Equation A.2 into Equation 6, the following partial differential equation is obtained as

$$r^2 \left(\partial^2 u_z / \partial r^2 \right) + r \left(\partial u_z / \partial r \right) + \lambda^2 \left(\partial^2 u_z / \partial \theta^2 \right) = 0 \quad (\text{A.3})$$

where $\lambda^2 = G_{\theta z} / G_{rz}$. Solving the partial differential given in Equation A.3 gives us

$$u_z(r, \theta) = \left(D_1 r^\lambda + D_2 r^{-\lambda} \right) \cos \theta. \quad (\text{A.4})$$

where D_1 and D_2 are the unknown constants. The displacement field shown in Equation A.4 is admissible since it satisfies the equilibrium equations.

A.2. Transverse shear deformation

The specific transverse shear loading condition is shown in Figure A.2 below, in which the general solutions of displacement functions are assumed to have the following form

$$u_r = u(r)\sin 2\theta, \quad u_\theta = w(r)\cos 2\theta, \quad u_z = 0. \quad (\text{A.5})$$

where $u(r)$ and $w(r)$ are some unknown functions that depends on the radius of RVE only.

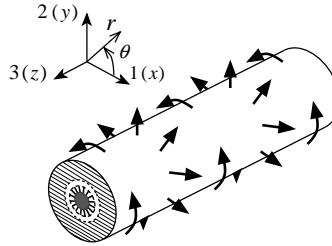


Figure A.2. Transverse shear loading condition

Substituting Equation A.5 into Equation 5, the relations of strain-displacement are obtained as

$$\begin{aligned} \varepsilon_{rr} &= u'(r)\sin 2\theta, \\ \varepsilon_{\theta\theta} &= \left((u(r) - 2w(r))/r \right) \sin 2\theta, \\ 2\varepsilon_{r\theta} &= \left((2u(r) - w(r))/r + w'(r) \right) \cos 2\theta. \end{aligned} \quad (\text{A.6})$$

where superscript prime notation represents derivative with respect to variable r . The subsequent substitution of Equation A.6 into Equation 1 provides us the stress-strain relationships, which can be written as

$$\begin{aligned} \sigma_{rr} &= \left[C_{rr}u'(r) + C_{r\theta}(u(r) - 2w(r))r^{-1} \right] \sin 2\theta, \\ \sigma_{\theta\theta} &= \left[C_{r\theta}u'(r) + C_{\theta\theta}(u(r) - 2w(r))r^{-1} \right] \sin 2\theta, \\ \sigma_{r\theta} &= G_{r\theta} \left((2u(r) - w(r))r^{-1} + w'(r) \right) \cos 2\theta. \end{aligned} \quad (\text{A.7})$$

Finally, substituting Equation A.7 into Equation 6, the two partial differential equations are obtained and expressed as

$$C_{rr} \left((r^2 u''(r) + ru'(r)) \right) - (C_{\theta\theta} + 4G_{r\theta})u(r) - 2(C_{r\theta} + G_{r\theta})rw'(r) + 2(C_{\theta\theta} + G_{r\theta})w(r) = 0 \quad (\text{A.8})$$

$$2(C_{r\theta} + G_{r\theta})ru'(r) + 2(C_{\theta\theta} + G_{r\theta})u(r) + G_{r\theta} \left(r^2 w''(r) + rw'(r) \right) - (4C_{\theta\theta} + G_{r\theta})w(r) = 0 \quad (\text{A.9})$$

Next, it is proposed that the general solutions to the second order partial differential equations given in Equation A.8 and Equation A.9 have the following solutions

$$u(r) = Fr^\lambda, \quad w(r) = Dr^\lambda. \quad (\text{A.10})$$

where F and D are some constants that are dependent with each other. We are now required to determine the characteristic equation that will define the value of material constant λ so that nontrivial solutions exist for the second order partial differential equations when taking into account the relations given in Equation A.10. Substitute Equation A.10 together with their first and second derivatives functions into Equation A.8 and Equation A.9, the following expressions are found.

$$\begin{aligned} \left[C_{rr}\lambda^2 - (C_{\theta\theta} + 4G_{r\theta}) \right] F - \left[2(C_{r\theta} + G_{r\theta})\lambda - 2(C_{\theta\theta} + G_{r\theta}) \right] D &= 0, \\ \left[2(C_{r\theta} + G_{r\theta})\lambda + 2(C_{\theta\theta} + G_{r\theta}) \right] F + \left[G_{r\theta}\lambda^2 - (4C_{\theta\theta} + G_{r\theta}) \right] D &= 0. \end{aligned} \quad (\text{A.11})$$

It is possible to combine the two expressions given in Equation A.11 and represent them as one single equation as in Equation A.12.

$$C_{rr}G_{r\theta}\lambda^4 - \left[(C_{rr} + C_{\theta\theta} - 8C_{r\theta})G_{r\theta} + 4(C_{rr}C_{\theta\theta} - C_{r\theta}^2) \right] \lambda^2 + 9C_{\theta\theta}G_{r\theta} = 0 \quad (\text{A.12})$$

Notice that Equation A.12 has the same form as the characteristic equation given in Equation 27. Again, the solution to this equation will provide the values for the required material constants - $\lambda_1, \lambda_2, \lambda_3$ and λ_4 . The general forms of solutions to the second order partial differential equations can be written as

$$\begin{aligned} u(r) &= F_1 r^{\lambda_1} + F_2 r^{\lambda_2} + F_3 r^{\lambda_3} + F_4 r^{\lambda_4}, \\ w(r) &= D_1 r^{\lambda_1} + D_2 r^{\lambda_2} + D_3 r^{\lambda_3} + D_4 r^{\lambda_4}, \end{aligned} \quad (\text{A.13})$$

where, as mentioned earlier, $\lambda_1^{(i)}$ and $\lambda_3^{(i)}$ are found to have real positive values and for $\lambda_2^{(i)}$ and $\lambda_4^{(i)}$, are real negative values. Since the unknown constants of F_j and D_j are dependent with each other, their relationships can be represented in the form of

$$F_j = \phi_j D_j \quad (\text{A.14})$$

where $\phi_j = 2 \left(C_{\theta\theta} + G_{r\theta} - \lambda_j (C_{r\theta} + G_{r\theta}) \right) \left(C_{\theta\theta} + 4G_{r\theta} - (\lambda_j)^2 C_{rr} \right)^{-1}$. Based on Equation A.14, Equation A.13 and Equation A.5, the final form of admissible displacement fields under transverse shear loading conditions can be expressed as

$$u_r(r) = \left(\sum_{j=1}^4 \phi_j D_j r^{\lambda_j} \right) \sin 2\theta, \quad u_\theta(r) = \left(\sum_{j=1}^4 D_j r^{\lambda_j} \right) \cos 2\theta. \quad (\text{A.15})$$

Note that the expressions shown in Equation A.15 are identical to the forms given in Equation 26.

B. Transformation equations

For main fibre material, the transformation equations from the engineering stiffness constants obtained from the experiments to elastic stiffness constants for transversely isotropic medium with its plane of symmetry perpendicular to the z-axis are provided as follows:

$$\begin{aligned} C_{11} &= C_{22} = C_{rr} = C_{\theta\theta} = E_T (1 - \nu_{TL} \nu_{LT}) \Upsilon, \\ C_{33} &= C_{zz} = E_L (1 - \nu_T^2) \Upsilon, \quad C_{12} = C_{r\theta} = E_T (\nu_T + \nu_{TL} \nu_{LT}) \Upsilon, \\ C_{13} &= C_{23} = C_{rz} = C_{\theta z} = E_T (\nu_{LT} + \nu_T \nu_{LT}) \Upsilon = E_L (\nu_{TL} + \nu_T \nu_{LT}) \Upsilon, \\ C_{44} &= C_{55} = G_{rz} = G_{\theta z} = \mu_L, \quad C_{66} = G_{r\theta} = \mu_T. \end{aligned} \quad (\text{B.1})$$

where $\Upsilon = (1 - \nu_T^2 - 2\nu_{TL} \nu_{LT} - 2\nu_T \nu_{TL} \nu_{LT})^{-1}$, $E_T = E_{11} = E_{22} = E_{rr} = E_{\theta\theta}$ - transverse Young's modulus, $E_L = E_{33} = E_{zz}$ - axial Young's modulus, $\nu_T = \nu_{12} = \nu_{21} = \nu_{r\theta} = \nu_{\theta r}$ - transverse Poisson's ratio, $\nu_{LT} = \nu_{31} = \nu_{32} = \nu_{rz} = \nu_{z\theta}$ - major Poisson's ratio, $\nu_{LT} = \nu_{13} = \nu_{23} = \nu_{rz} = \nu_{\theta z}$ - minor Poisson's ratio, $\mu_L = \mu_{13} = \mu_{31} = \mu_{23} = \mu_{32} = \mu_{rz} = \mu_{zr} = \mu_{\theta z} = \mu_{z\theta}$ - axial shear modulus and $\mu_T = \mu_{12} = \mu_{21} = \mu_{r\theta} = \mu_{\theta r} = E_T / 2(1 + \nu_T)$ - transverse shear modulus. Further useful relations are given as follows: $\nu_{31} / E_{33} = \nu_{13} / E_{11}$, $\nu_{32} / E_{33} = \nu_{23} / E_{22}$.

For reinforced interphase layer, the transformation equations for transversely isotropic medium with its axis of symmetry parallel to the r-axis are given as follows:

$$\begin{aligned} C_{11} &= C_{rr} = E_{11}^{eff-lnt} + 4(\nu_{12}^{eff-lnt}) K_{23}^{eff-lnt}, \\ C_{12} &= C_{13} = C_{r\theta} = C_{rz} = 2K_{23}^{eff-lnt} \nu_{12}^{eff-lnt}, \\ C_{22} &= C_{33} = C_{\theta\theta} = C_{zz} = \mu_{23}^{eff-lnt} + K_{23}^{eff-lnt}, \\ C_{23} &= C_{\theta z} = -\mu_{23}^{eff-lnt} + K_{23}^{eff-lnt}, \\ C_{66} &= C_{55} = G_{r\theta} = C_{rz} = \mu_{12}^{eff-lnt} = \mu_{13}^{eff-lnt}. \end{aligned} \quad (\text{B.2})$$

As for isotropic matrix or other constituent material, the following relations are defined as

$$\begin{aligned} C_{11} = C_{22} = C_{33} = C_{rr} = C_{\theta\theta} = C_{zz} &= E(1-\nu)/(1+\nu)(1-2\nu), \\ C_{12} = C_{13} = C_{23} = C_{r\theta} = C_{rz} = C_{\theta z} &= E\nu/(1+\nu)(1-2\nu) \end{aligned} \quad (\text{B.3})$$

and the shear modulus can be defined as $\mu = E/2(1+\nu)$.

Acknowledgement

The principle author is highly indebted to Prof Dr Sergey Lurie and Dr Natasha Tuchkova, Institute of Applied Mechanics, Russian Academy of Sciences, Moscow for the fruitful discussion in this research area and the supports they have extended throughout these years.

References

- [1] Baur J and Silverman E 2007 *MRS Bulletin* **32** 328-34
- [2] Gibson R E 2010 *Compos. Struct.* **92** 2793-810
- [3] Lin Y, Ehlert G J and Sodano H A 2009 *Adv. Funct. Mater.* **19** 2654-60
- [4] Agnihotri P, Basu S and Kar K K 2011 *Carbon* **49** 3098-106
- [5] Liao Q, Zhang Z, Zhang X, Mohr M, Zhang Y, Fecht H-J 2014 *Nano Research* **7** 917-28
- [6] Garcia E J, Wardle B L, Hart A J and Yamamonoj N 2008 *Compos. Sci. Technol.* **68** 2034-41
- [7] Steiner S A, Li R and Wardle B L 2013 *ACS Appl. Mater. Interf.* **5** 4892-903
- [8] Yamamoto N, Villoria R G and Wardle B L 2012 *Compos. Sci. Technol.* **72** 2009-15
- [9] Lurie S and Minhat M 2014 *Compos. B* **61** 26-40
- [10] Guz I A, Rodger A A, Guz A N and Rushchitsky J J 2008 *Philos Trans R Soc A* **366** 1827-33
- [11] Hashin Z and Rosen B W 1964 *J. Appl. Mech.* **31** 223-32
- [12] Hill R 1965 *J. Mech. Phys. Solids* **13** 213-22
- [13] Christensen R M and Lo K H 1979 *J. Mech. Phys. Solids* **27** 315-30
- [14] Norris A N 1985 *Mech. Mater.* **4** 1-16
- [15] Benveniste Y, Dvorak G J and Chen T 1987 *Mech. Mater.* **6** 147-57
- [16] Christensen R M 1990 *J. Mech. Phys. Solids* **38** 379-404
- [17] Lurie S, Minhat M, Tuchkova N and Soliaev J 2014 *Appl. Compos. Mater.* **21** 179-96
- [18] Nemat-Nasser S and Hori M 1999 *Micromechanics: Overall properties of heterogeneous materials* (Amsterdam: Elsevier)
- [19] Aboudi J, Arnold S M and Bednarczyk B A 2013 *Micromechanics of composite materials: A generalized multiscale analysis approach* (Oxford, Massachusetts: Butterworth-Heinemann)
- [20] Herve E and Zaoui 1995 *Int. J. Eng. Sci.* **33** 1419-33
- [21] Norris A N 1989 *J. Appl. Mech.* **56** 83-8
- [22] Hashin Z 2002 *J. Mech. Phys. Solids* **50** 2509-37
- [23] Lurie S and Minhat M 2014 *Compos. B* **61** 26-40
- [24] Lurie S, Minhat M. and Tuchkova N 2015 *J. Eng. Math.* **95** 7-29
- [25] Ehlert G J 2012 *Development of zinc oxide nanowire interphase for enhanced structural composites* PhD Thesis University of Florida
- [26] Chatzigeorgiou G, Efendiev Y and Lagoudas D C 2011 *Int. J. Solids Struct.* **48** 2668-80
- [27] Pozegic T R, Hamerton I, Anguita J V, Tang W, Balocchi P, Jenkins P and Silva S R P 2014 *Carbon* **74** 319-28